Liquid Crystals
Publication details, including instructions for authors and subscription information:
http://www.informaworld.com/smpp/title~content=t713926090

DTA, X-ray and dielectric relaxation studies of 14CB at atmospheric and elevated pressures

Stanisław Urban[a]; Albert Würflinger[b]; Bo Gestblom[c]; Roman Dąbrowski[d]; Jan Przedmojski[e]
[a] M. Smoluchowski Institute of Physics, Jagiellonian University, Reymonta 4, 30-059 Kraków, Poland, [b] Physical Chemistry II, Ruhr University, D-44780 Bochum, Germany, [c] Institute of Physics, Uppsala University, S-75121 Uppsala, Sweden, [d] Institute of Chemistry, Military University of Technology, 00-908 Warsaw, Poland, [e] Institute of Physics, Technical University, Warsaw, Poland,

To cite this Article Urban, Stanisław , Würflinger, Albert , Gestblom, Bo , Dąbrowski, Roman and Przedmojski, Jan(2003) 'DTA, X-ray and dielectric relaxation studies of 14CB at atmospheric and elevated pressures', Liquid Crystals, 30: 3, 305 — 311

To link to this Article: DOI: 10.1080/0267829031000068657

URL: http://dx.doi.org/10.1080/0267829031000068657

LIQUID CRYSTALS, 2003, VOL. 30, NO. 3, 305–311

Taylor & Francis
Taylor & Francis Group

DTA, X-ray and dielectric relaxation studies of 14CB at atmospheric and elevated pressures

STANISŁAW URBAN*
M. Smoluchowski Institute of Physics, Jagiellonian University, Reymonta 4,
30-059 Kraków, Poland

ALBERT WÜRFLINGER
Physical Chemistry II, Ruhr University, D-44780 Bochum, Germany

BO GESTBLOM
Institute of Physics, Uppsala University, S-75121 Uppsala, Sweden

ROMAN DĄBROWSKI
Institute of Chemistry, Military University of Technology, 00-908 Warsaw, Poland

and JAN PRZEDMOJSKI
Institute of Physics, Technical University, Warsaw, Poland

(*Received 1 July 2002; in final form 1 October 2002; accepted 18 October 2002*)

The pressure–temperature phase diagram of 4′-tetradecyl-4-cyanobiphenyl (14CB) up to 220 MPa (2.2 kbar) and between 320–400 K was established using DTA. The temperature range of the smectic A (SmA) phase slightly increases with pressure. The layer spacing d at 1 atm was determined as a function of temperature using X-ray diffraction. It was related to the molecular length l by the ratio $d/l \sim 1.4$. The dielectric relaxation measurements in the isotropic and smectic A_d phases of 14CB at 1 atm were performed in the frequency range 10 kHz–3 GHz. Contributions from both principal rotational motions, i.e. around the short and long molecular axes, were separated. The relaxation measurements under high pressure in the SmA phase covered the low frequency process. The longitudinal relaxation time τ_1, characterizing the molecular reorientations around the short axis, was analysed with respect to the pressure and temperature dependences, giving activation volumes, $\Delta^{\#}V = RT(\partial \ln \tau_1/\partial p)_T$, and activation enthalpies, $\Delta^{\#}H = RT(\partial \ln \tau_1/\partial T^{-1})_p$, respectively. Surprisingly, all the activation quantities characterizing the rotational motions of 14CB molecules under different conditions are nearly the same as those determined recently for the much shorter homologue, 8CB. This indicates that the 14CB molecule is in fact relatively short due to conformational motions of the alkyl tail.

1. Introduction

The 4′-alkyl-4-cyanobiphenyls (nCBs) are liquid crystalline (LC) substances first discovered in the 1970s [1, 2]. The first four nematogenic members, $n = 5$–8, have been intensively studied using various experimental techniques. They were considered as model compounds with which to test theoretical models and because of their physical properties are also of interest from an applications viewpoint. The higher members of the series were not considered to be so interesting as they have only a narrow nematic range (9CB) or are purely smectogenic. Nevertheless, in order to investigate the influence of the length of the alkyl chain on the phase behaviour and molecular dynamics, we have undertaken studies of the nCBs with $n \geqslant 9$. As a first step the pressure–temperature, p–T, phase diagrams were established for the homologues with $n = 9$–12 [3]. A pressure-induced nematic (N) phase was found for 10CB and 11CB below 200 MPa. Some interesting information about the clearing transitions, either I → N or I → SmA, as a function

---

*Author for correspondence; e-mail: ufurban@cyf-kr.edu.pl

Liquid Crystals ISSN 0267-8292 print/ISSN 1366-5855 online © 2003 Taylor & Francis Ltd
http://www.tandf.co.uk/journals
DOI: 10.1080/0267829031000068657

of pressure for the compounds with $n = 5$–12 come from the non-linear dielectric effect (NDE) studies by Drozd-Rzoska *et al.* [4]. The present investigation of 14CB, the longest member of the *n*CB series synthesized, was performed with the aims to establish the *p*–*T* phase diagram up to 250 MPa using differential thermal analysis (DTA), to determine the layer spacing in the smectic phase by X-ray measurements, and to study the rotational dynamics of molecules in the isotropic (I) and smectic A_d (SmA_d) phases at atmospheric and elevated pressures using broad band dielectric spectroscopy. The relaxation times, activation enthalpies and activation volumes obtained will be discussed together with those of the much shorter member, 8CB, in the I, N and SmA_d phases [5, 6]. In particular, the low frequency relaxation process, associated with molecular rotations around the short axes, should be sensitive to the length of the alkyl chain.

2. Experimental

14CB was synthesized in the Institute of Chemistry, Military University of Technology, Warsaw. The 4′-alkyl-4-cyanobiphenyls are commercially produced by treating 4′-alkyl-4-bromobiphenyls with CuCN [7, 8]. On a laboratory scale, 4′-alkyl-4-iodobiphenyls are more convenient intermediates, because only mild conditions are required for the reaction involving halogen exchange [9]. Both these methods give pure products for compounds having short alkyl chains, but not for homologues containing longer chains because of the difficulty in the separation of pure 4′-alkyl-4-bromobiphenyls or 4′-alkyl-4-iodobiphenyls. For this reason we decided to prepare 14CB (and also 9CB, 10CB, 11CB and 12CB [3]), by the method shown in the scheme. We had previously tested this route in the synthesis of 5CB [10], but because it was much longer than that making use of the iododerivatives, we did not recommend it for the preparation of short chain compounds. The details of the syntheses of the compounds 9CB–14CB are the same as described for 5CB, with only the difference that the reduction of the ketones (3) was achieved using hydrogen in the presence of a Pd/C catalyst instead of by using hydrazine. The reduction of the very long ketones (3) using Wolff–Kishner conditions did not give good yields. The final compound was dissolved in hexane, filtered through a silica gel layer and cooled to −20°C to obtain crystals. The purity of 14CB was 99.3% (GC) or 99.2% (DSC); the main impurity was 16CB. The transition temperatures measured on heating are:

$$\mathrm{Cr} \rightarrow 55.2^{\circ}\mathrm{C} \rightarrow \mathrm{SmA} \rightarrow 61.9^{\circ}\mathrm{C} \rightarrow \mathrm{I}$$

The enthalpy changes associated with these transitions are 41.7 kJ mol^{-1} for melting and 5.72 kJ mol^{-1} for clearing.

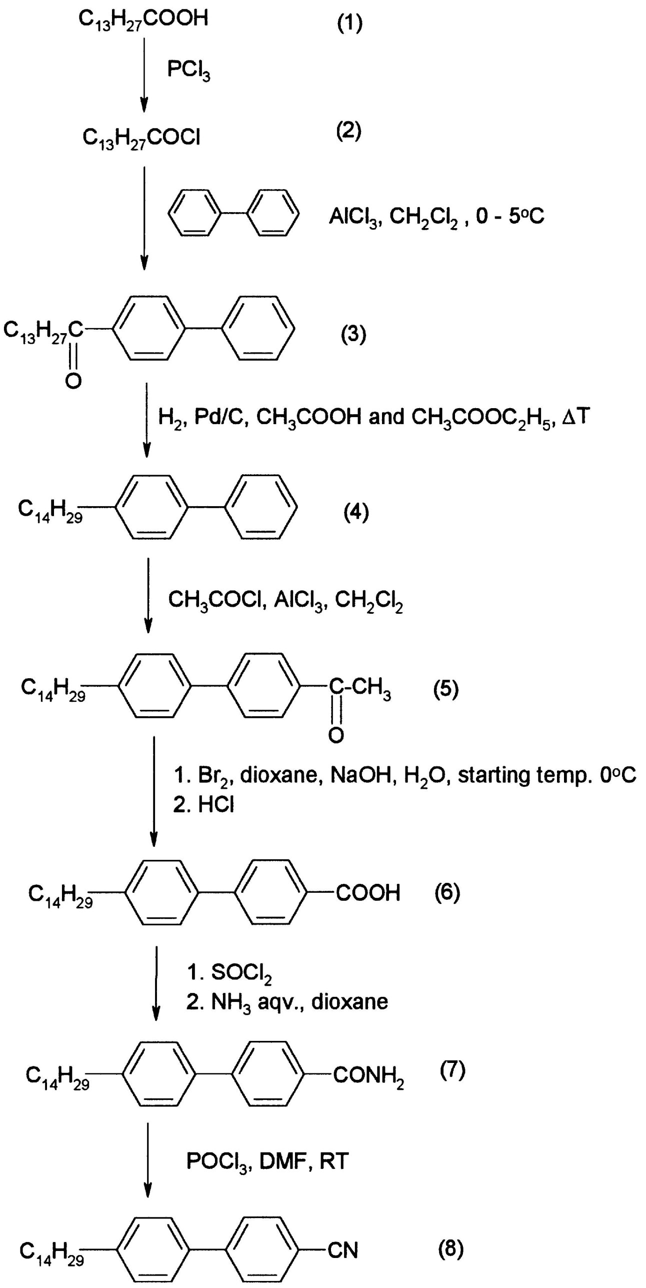

Scheme. Synthesis of 14CB.

DTA measurements were performed at the Ruhr University of Bochum. Two high pressure DTA instruments have been used which were constructed for measurements at low [11] and high [12] temperatures. DTA peaks were generated at heating rates of 1 K min^{-1} and recorded using a two-channel recorder.

The X-ray scattering measurements were performed at the Technical University, Warsaw, using a DRON-UM2 diffractometer, with Cu radiation monochromatized by a flat Ge crystal. The first order Bragg peaks corresponding to the layer thicknesses were measured using the conventional 2*q*-*q* method. A computer programme organized the step *q*-scans, collected counts and calculated the layer spacing and the breadth of the peak. A thin layer of the sample was aligned on a glass substrate by cooling from the isotropic phase. This procedure was similar to that described elsewhere [13]. The temperature was stabilized to within ± 0.1 K.

The dielectric relaxation studies in the isotropic phase of 14CB were performed at Uppsala University using a time domain spectroscopy method as described elsewhere [14]. The 50 ns time window was applied which covers the frequency band from *c.* 20 MHz to *c.* 3 GHz. The low frequency relaxation process in the SmA phase was studied at 1 atm in Kraków and at elevated pressures in Bochum. The experimental procedures were the same as those described previously [5, 6, 15–17]. No influence of a d.c. electric field (~ 3000 V cm^{-1}) on the permittivity values in the SmA phase was detected.

3. Results

3.1. *DTA studies*

Figure 1 presents the *p*–*T* phase diagram constructed for 14CB. The insert shows a typical DTA trace. Up to 220 MPa the SmA–I (T_{cl}) and Cr–SmA (T_m) transition lines, can be expressed by the polynomials (T/K, p/MPa):

$$T_{cl} = 335.6 + 0.297p - 1.415 \times 10^{-4} p^2$$

$$T_m = 328.3 + 0.265p - 1.66 \times 10^{-4} p^2.$$

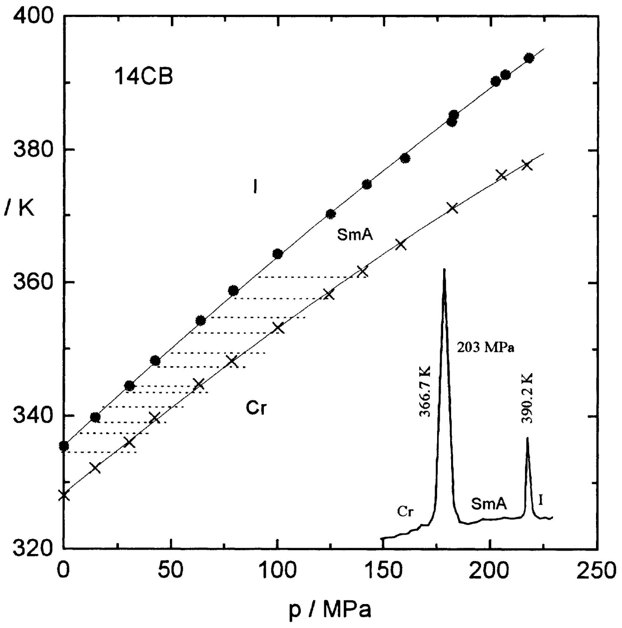

Figure 1. Pressure–temperature phase diagram for 14CB. Horizontal dotted lines indicate the temperatures at which the dielectric relaxation measurements were performed. The insert shows a typical DTA trace.

No splitting of the clearing line $T_{cl}(p)$ was observed for 14CB, unlike for the two shorter members, 10CB and 11CB [3], and other similar compounds [16, 17].

3.2. *X-ray studies*

Figure 2 presents the layer spacing *d* in the SmA phase of 14CB as a function of temperature. A linear increase of *d* within the smectic phase was observed down to the crystallization of the sample.

3.3. *Dielectric studies at ambient pressure*

The spectra of the isotropic phase of 14CB plotted in the form of Cole–Cole diagrams are skewed on the high frequency side (figure 3) which is typical for all cyano-compounds [5, 18]. As in previous studies [5, 18] we assume that this results from a superposition of two relaxation processes connected with the principal rotational motions of the molecules: specifically, around the short axis (the low frequency l.f. process) and around the long axis (the high frequency h.f. process). Both these motions contribute to the dielectric spectrum due to an inclination by an angle β of the dipole moment away

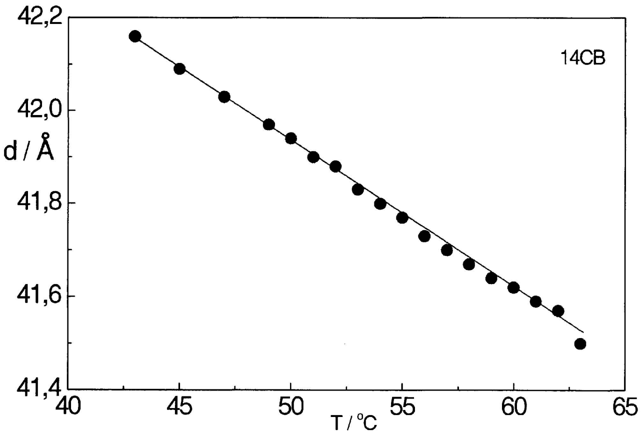

Figure 2. The layer spacing as a function of temperature in the SmA phase of 14CB.

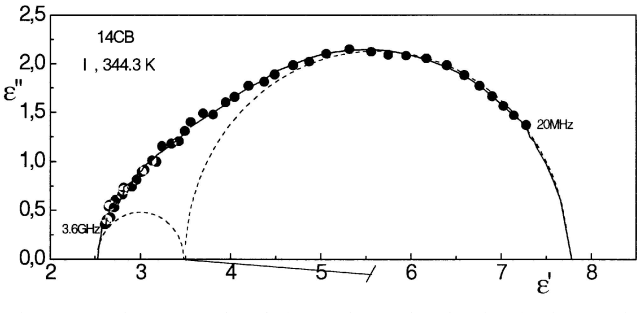

Figure 3. An example of the Cole–Cole plot in the isotropic phase of 14CB. The solid line is the fit using two relaxation processes given by equation (1) which are depicted by the dashed arcs of circles.

from the lowest inertia moment axis caused by the conformational motions of the alkyl chain. Thus, the measured spectra were analysed using the equation

$$\varepsilon^*(\omega)-\varepsilon_\infty=\frac{\delta_1}{(1+\mathrm{i}\omega\tau_1)^{1-\alpha_1}}+\frac{\delta_2}{(1+\mathrm{i}\omega\tau_2)^{1-\alpha_2}} \qquad (1)$$

where $\varepsilon^*=\varepsilon'-\mathrm{i}\varepsilon''$ is the complex dielectric permittivity; $\delta_1=\varepsilon_s-\varepsilon_2$ and $\delta_2=\varepsilon_2-\varepsilon_\infty$, are the strengths (increments) of both relaxation processes; ε_s and ε_∞ are the static and high frequency permittivities, respectively, and α characterizes a distribution of the relaxation times. The best and most consistent fits over a broad temperature interval were obtained assuming $\alpha_2=0$ which gave $\alpha_1\approx 0.03$–0.05 and the relaxation times shown in figure 5. As expected, the increment δ_1 corresponding to the slower process is distinctly larger than δ_2 characterizing the faster process, as they have to be related to the longitudinal and transverse components of the dipole moment ($\delta\sim\mu^2$), respectively. The static permittivity in the isotropic phase of 14CB, $\varepsilon_{s,I}\approx 7.8$, is markedly smaller than that measured for the shorter members of the *n*CB series [5, 6, 15, 19–21]. The relaxation times $\tau_1=\tau_{\mathrm{l.f.}}$ and $\tau_2=\tau_{\mathrm{h.f.}}$ are shown in figure 5 in the form of the Arrhenius plots. The slopes of the lines fitted to the experimental points give the activation enthalpies according to $\Delta^{\#}H=R(\partial\ln\tau/\partial T^{-1})$ where R is the gas constant. Thus, $\Delta^{\#}H^{\mathrm{I}}_{\mathrm{l.f.}}=35.3\pm2\,\mathrm{kJ\,mol^{-1}}$ and $\Delta^{\#}H^{\mathrm{I}}_{\mathrm{h.f.}}=23.0\pm3\,\mathrm{kJ\,mol^{-1}}$. Both these values are close to those determined for other similar substances but containing, however, markedly shorter terminal chains [5, 15, 22].

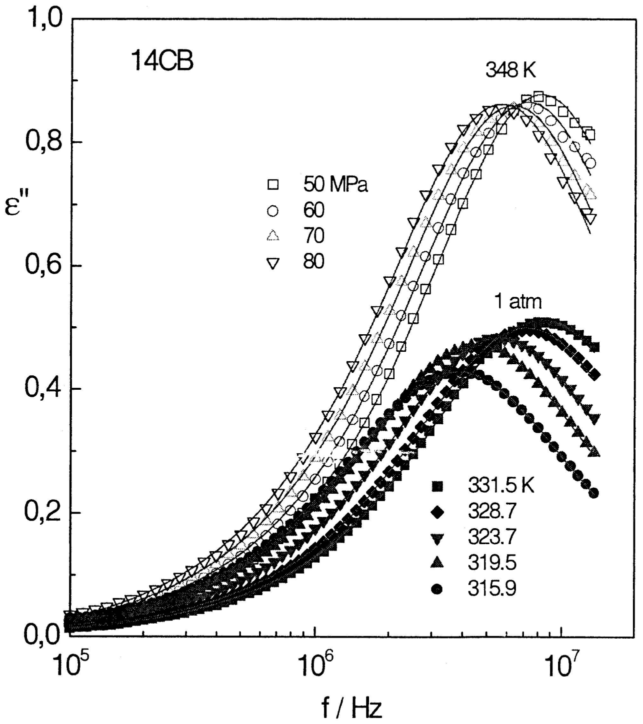

Figure 4. Examples of the absorption spectra collected in the SmA phase of 14CB at atmospheric pressure and different temperatures, and at constant temperature (348 K) under various pressures.

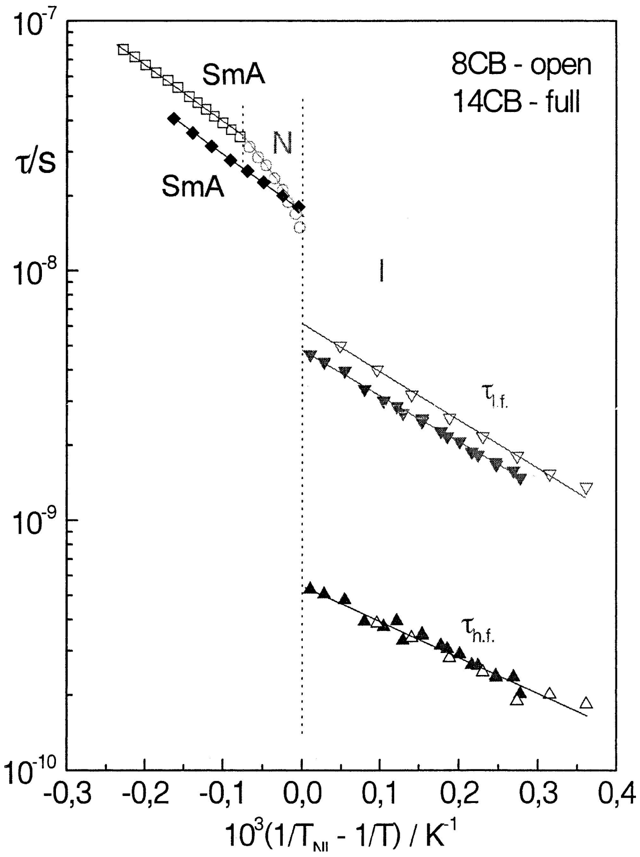

Figure 5. Arrhenius plots for the relaxation processes observed at 1 atm in the isotropic and smectic A phases of 14CB (filled symbols), and for 8CB in the isotropic, nematic and smectic A phases (open symbols). The temperature scale was chosen in order to avoid shifts caused by the different clearing temperatures of the compounds.

The permittivity dropped considerably at the I–SmA transition for 14CB (from *c.* 7.9 to *c.* 4.8); this effect is connected with the lack of alignment of the sample. In spite of this fact, however, the relaxation spectra can be described well using the Debye equation, i.e. one part of equation (1) with $\alpha=0$. Undoubtedly, the relaxation process observed is associated with the molecular reorientations around the short axis. Examples of the absorption spectra are shown in figure 4. The l.f. relaxation times $\tau_{\mathrm{l.f.}}$ were calculated from the frequency corresponding to the maximum of absorption: $\tau_{\mathrm{l.f.}}=1/(2\pi f_{\mathrm{max}})$ and are shown in figure 5. The slowing down of the l.f. relaxation process can be characterized using a retardation factor, $g_{\mathrm{A\text{-}I}}=\tau_{\mathrm{A}}/\tau_{\mathrm{I}}$ taken at the clearing point. Thus $g_{\mathrm{A\text{-}I}}=3.32$, and this value is very close to the $g_{\text{N-I}}$ factors determined for nematogenic members of the series [5]. The activation enthalpy $\Delta^{\#}H^{A} = 43.4 \pm 2\,\text{kJ mol}^{-1}$ is identical to that found for the much shorter homologue, 8CB, in the SmA phase [6, 20, 23].

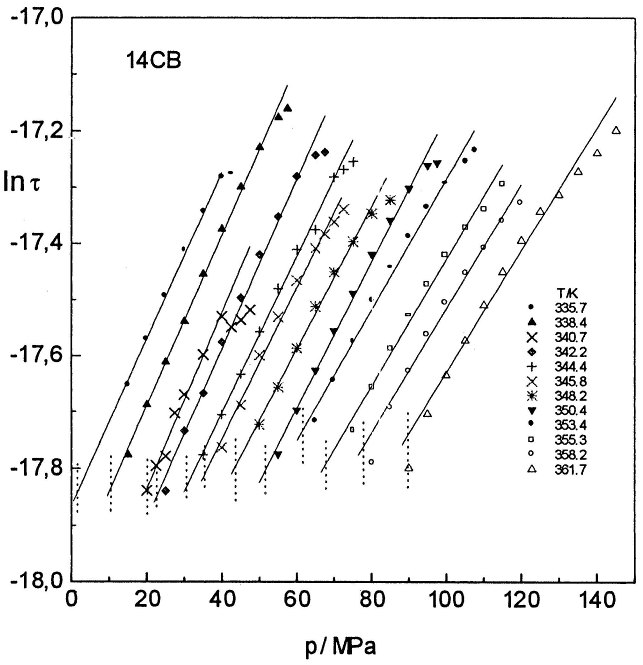

Figure 6. Logarithm of the longitudinal relaxation time versus pressure for the SmA phase of 14CB at different temperatures. The slopes of the lines yield the activation volumes shown in figure 7 (*a*). The vertical dotted lines mark the clearing temperatures.

It is markedly smaller, however, than the values characterizing the molecular rotations around the short axes in the N phase of two-ring compounds [5, 6, 15, 20, 23].

The relaxation times for 14CB are compared with those obtained for 8CB under the same experimental conditions in figure 5. The data for 8CB are in good agreement with those reported by Druon and Wacrenier [20] and Buka and Price [23].

3.4. *Dielectric measurements at elevated pressures*

In general these measurements were performed while decreasing the pressure at constant temperature. The permittivity values were greater than those measured at ambient pressure. In figure 4 examples of the absorption spectra collected at constant temperature but different pressures are shown. The Debye equation describes the spectra very well. The logarithm of the l.f. relaxation times calculated from $f_{\max}$ are shown in figure 6 as a function of pressure for various temperatures. From the slopes of the lines fitted to the points, the activation volume, $\Delta^{\#}V = RT(\partial \ln \tau/\partial p)_T$, was calculated and shown in figure 7 (*a*). By taking the data shown in figure 6 at constant pressures, we also calculated the activation enthalpies, $\Delta^{\#}H = R(\partial \ln \tau/\partial T^{-1})_p$, which are shown in figure 7 (*b*).

4. Discussion

The X-ray and dielectric measurements were performed with decreasing temperature. Due to supercooling, the temperature range of the SmA phase was

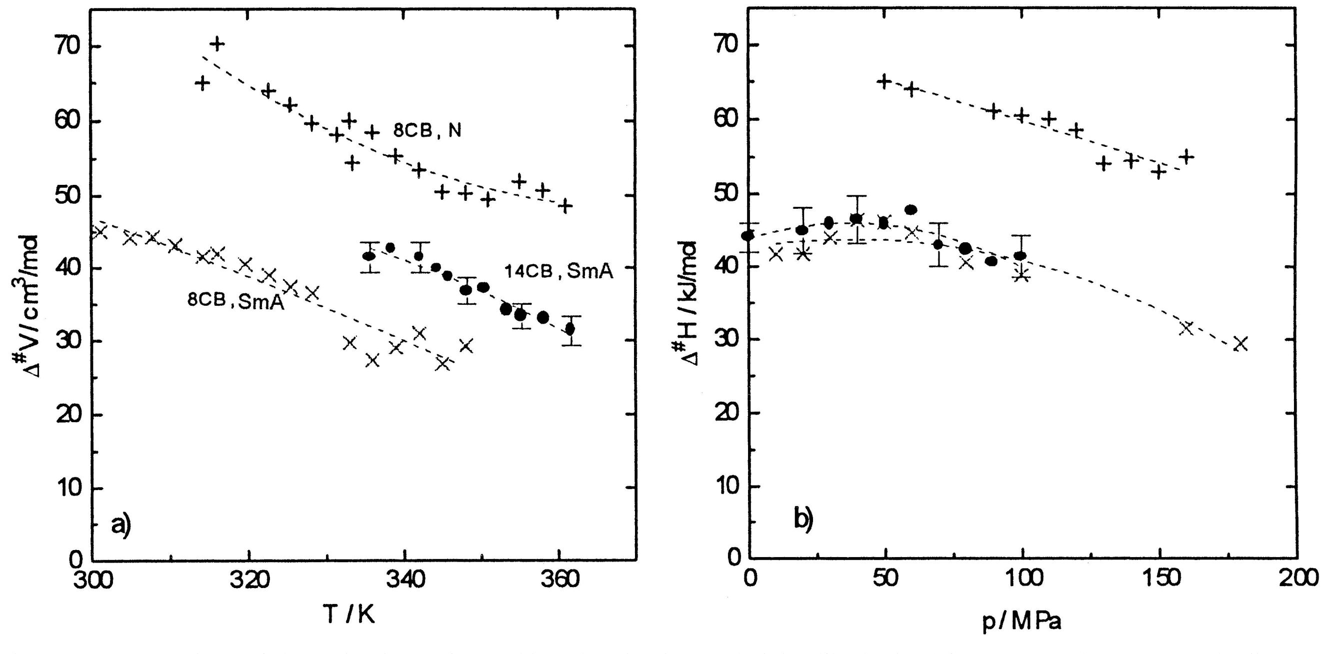

Figure 7. Comparison of the activation volumes (*a*) and activation enthalpies (*b*) obtained for 14CB and 8CB [6]. The lines are guides for the eye only.

considerably extended (from *c.* 7 K to *c.* 20 K). This allows for greater confidence in the observed trends in the behaviour of the measured quantities.

The layer spacing measured for 14CB in the SmA phase may be compared with the data reported for the shorter members of the series: 5CB and 7CB in the N phase [24]; 8CB, 10CB, 12CB [25]; 6CB (N), 12CB [26]; 9CB [27]; and 8CB, 12CB [28]. Estimates of the lengths *l* of the molecules in the most extended conformation of the alkyl chains confirm that the layer spacings are incommensurate with the molecular lengths. Figure 8 shows the *d* and *l* values and their ratio for several members of the *n*CBs. In the case of 14CB the molecular length was calculated using HyperChem. Taking into account the lengths of the chemical bonds and the van der Waals radii of terminal atoms, $l = 30.9$ Å. This value correlates well with the lengths of the other members of the series, see figure 8 (*b*). Thus, the d/l ratio varies between 1.34 and 1.36 within the SmA phase of 14CB and is rather smaller than predicted if one extrapolates the ratios observed for the shorter smectogenic members, figure 8 (*c*). Two factors must be taken into account when discussing this effect: firstly, antiparallel correlations of the molecules are a characteristic feature for all cyano compounds [24–31]; secondly, the conformational motions of the alkyl chain may considerably shorten the molecule and make it more bulky. Considering all the arguments of other researchers [24–31], we think that in the antiparallel dimer the biphenyl cores overlap giving $d_{\mathrm{calc}} \sim 45.1$ Å which is larger than the experimental values (figure 2). An additional decrease of *d* must be due to the conformational motions of the tetradecyl chains, a conclusion which appears to be supported by the dielectric results.

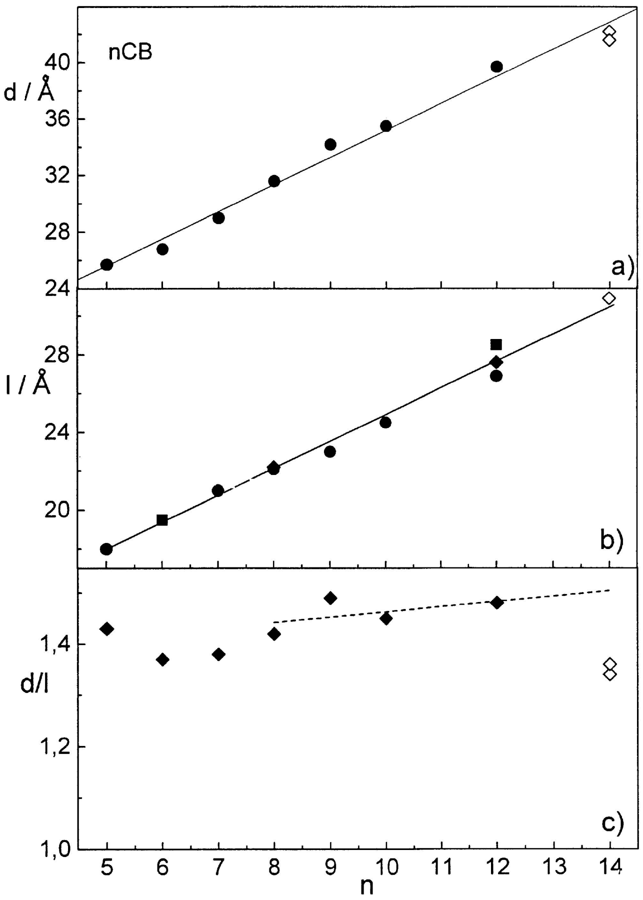

Figure 8. (*a*) The layer thickness *d*, (*b*) the length of the molecules in their most extended conformation *l*, (*c*) and the ratio *d*/*l* for several members of the *n*CB series. The data for 14CB correspond to the lower and upper temperatures (see figure 2).

Taking into account the Onsager equation,

$$\mu^2 = \frac{9kT\varepsilon_0(\varepsilon_s - \varepsilon_\infty)(2\varepsilon_s + \varepsilon_\infty)}{N\varepsilon_s(\varepsilon_\infty + 2)^2} \qquad (2)$$

and the increments $\varepsilon_s - \varepsilon_2$ and $\varepsilon_2 - \varepsilon_\infty$ from figure 2, we can estimate the ratio of the transverse and longitudinal components of the dipole moment $\mu_t/\mu_l = \tan\beta$ (ε_o is the free space permittivity and *N* is the number density). Thus the calculated value of β is 34° and is in good agreement with the angle of $\sim 32°$ estimated from the extrapolation of β-values determined in the same way for *n*CBs with $n = 5$–8 [5]. This means that the longer the alkyl chain the larger is the inclination of the dipole moment from the long axes. This is caused by the increasing number of conformers associated with increasing chain length.

Another manifestation of this effect can be deduced from comparisons of the relaxation data obtained for 8CB and 14CB. The relaxation times obtained at ambient pressure for both compounds are compared in figure 5. As can be seen, the l.f. relaxation process has almost the same relaxation times and activation enthalpies in all the phases studied, despite, the very different molecular lengths, and thus probably large differences in the values of the momentum of inertia for the molecular rotation around the short axes. The similarity of the activation volumes for both compounds in the SmA phase, figure 7 (*a*), means that the free volume necessary for the rotational jumps over the barrier are comparable for molecules having very different lengths. In turn, the equality of the activation enthalpies, figure 7 (*b*) indicates that the interaction energy between molecules arises from the rigid cyanobiphenyl cores rather than from the whole molecules. These experimental data indicate that the 14CB molecule has a much bulkier shape than expected if the alkyl chains were to adopt the all-*trans* conformation.

5. Conclusions

The analysis of the data showed that: (1) The layer spacing in the SmA phase of 14CB is incommensurate with the molecular length as for other cyano compounds. (2) The molecules form antiparallel dimers in such a way that the molecular cores overlap. (3) The dipole moment of the molecule shows a large inclination with respect to the long molecular axis, characterized by the angle $\beta \approx 34^\circ$. (4) Similar values of the l.f. relaxation times and the corresponding activation parameters in the I and SmA phases of 8CB and 14CB, which have very different molecular lengths, indicate that the 14CB molecule has a much bulkier shape than expected if the alkyl chains adopted the all-*trans* conformation.

This work was sponsored in part by the Polish Government KBN Grant No 2 P03B 052 22.

References

[1] Gray, G. W., Harrison, K., and Nash, J. A., 1973, *Electron. Lett.*, **9,** 130.

[2] Demus, D., and Zaschke, H. (editors), 1984, *Flüssige Kristalle in Tabellen* (Leipzig: VEB).

[3] Urban, S., Massalska-Arodź, M., Würflinger, A., and Dąbrowski, R., 2003, *Liq. Cryst.*, **30,** 3, pp. 313–318.

[4] Drozd-Rzoska, A., Rzoska, S. J., and Zioło, J., 2000, *Phys. Rev. E*, **61,** 5349.

[5] Urban, S., Gestblom, B., and Würflinger, A., 1999, *Mol. Cryst. liq. Cryst.*, **331,** 113.

[6] Markwick, P., Urban, S., and Würflinger, A., 1999, *Z. Naturforsch.*, **54a,** 275.

[7] Gray, G. W., and Harrison, K. J., British Patent 1 433 130.

[8] Gray, G. W., and Mosley, A., 1976, *J. chem. Soc. Perkin Trans. II*, 97.

[9] Dąbrowski, R., Witkiewicz, Z., and Kenig, K., 1980, *Mol. Cryst. liq. Cryst.*, **58,** 251.

[10] Adamska, G., Dąbrowski, R., Dziaduszek, J., Kenig, K., and Żytyński, E., 1978, *Biul. WAT,* **27,** 91.

[11] Pingel, N., Poser, U., and Würflinger, A., 1984, *J. chem. Soc. Faraday Trans. I*, **80,** 3221.

[12] Schmidt, C., Rittmeier-Kettner, M., Becker, H., Ellert, J., Krombach, R., and Schneider, G. M., 1994, *Thermochim. Acta*, **238,** 321.

[13] Ikeda, A., Takanishi, Y., Takezoe, H., and Fukuda, A., 1993, *Jpn. J. appl. Phys.*, **32,** 497.

[14] Gestblom, B., and Wróbel, S., 1995, *Liq. Cryst.*, **18,** 31; Urban, S., Gestblom, B., and Dąbrowski, R., 1999, *Phys. Chem. chem. Phys.*, **1,** 4843.

[15] Urban, S., and Würflinger, A., 1997, *Adv. chem. Phys.*, **98,** 143.

[16] Urban, S., Würflinger, A., and Kocot, A., 2001, *Liq. Cryst.*, **28,** 1331.

[17] Würflinger, A., and Urban, S., 2001, *Phys. Chem. chem. Phys.*, **3,** 3727.

[18] Urban, S., Gestblom, B., Kresse, H., and Dąbrowski, R., 1996, *Z. Naturforsch.*, **51a,** 834.

[19] Dunmur, D. A., Manterfield, M. R., Miller, W. H., and Dunleavy, J. K., 1978, *Mol. Cryst. liq. Cryst.*, **45,** 127.

[20] Druon, C., and Wacrenier, J.-M., 1978, *Ann. Phys.*, **3,** 199.

[21] Jadżyn, J., and Kędziora, P., 1987, *Mol. Cryst. liq. Cryst.*, **145,** 17.

[22] Urban, S., Gestblom, B., and Dąbrowski, R., 1998, *Liq. Cryst.*, **24,** 681.

[23] Buka, A., and Price, A. H., 1985, *Mol. Cryst. liq. Cryst.*, **116,** 187.

[24] Leadbetter, A. J., Richardson, R. M., and Colling, C. N., 1975, *J. Physique Colloq.*, **36,** C1-37.

[25] Leadbetter, A. J., Frost, J. C., Gaughan, J. P., Gray, G. W., and Mosley, A., 1979, *J. Physique*, **40,** 375.

[26] Coles, H. J., and Strazielle, C., 1979, *Mol. Cryst. liq. Cryst. Lett.*, **49,** 259.

[27] Bradshaw, M. J., and Raynes, E. P., 1983, *Mol. Cryst. liq. Cryst.*, **91,** 145.

[28] Czupryński, K., and Januszko, A., 1992, *Mol. Cryst. liq. Cryst.*, **215,** 199.

[29] Brownsey, G. J., and Leadbetter, A. J., 1980, *Phys. Rev. Lett.*, **44,** 1608.

[30] Dąbrowski, R., Przedmojski, J., and Baran, J., 1986, *Cyst. Res. Techn.*, **21,** 567.

[31] Dąbrowski, R., Jadżyn, J., Przedmojski, J., and Baran, J., 1987, *Cyst. Res. Techn.*, **22,** 861.